AGU PUBLICATIONS

Global Biogeochemical Cycles

RESEARCH ARTICLE
10.1002/2014GB004858

Key Points:
- Vegetation plays a large role in Mn cycling in temperate forested ecosystems
- Vegetation dominated Mn cycling across pot, pedon, and watershed scales
- Biological recycling retains anthropogenic Mn deposited to watersheds

Supporting Information:
- Readme
- Equations (S1)–(S7), Figures S1–S4, and Tables S1–S3
- Table S1
- Table S2

Correspondence to:
E. M. Herndon,
eherndo1@kent.edu

Citation:
Herndon, E. M., L. Jin, D. M. Andrews, D. M. Eissenstat, and S. L. Brantley (2015), Importance of vegetation for manganese cycling in temperate forested watersheds, *Global Biogeochem. Cycles*, *29*, doi:10.1002/2014GB004858.

Received 21 MAR 2014
Accepted 19 JAN 2015
Accepted article online 23 JAN 2015

Importance of vegetation for manganese cycling in temperate forested watersheds

Elizabeth M. Herndon[1,2], Lixin Jin[3,4], Danielle M. Andrews[5], David M. Eissenstat[5], and Susan L. Brantley[1,3]

[1]Department of Geosciences, Pennsylvania State University, University Park, Pennsylvania, USA, [2]Now at Department of Geology, Kent State University, Kent, Ohio, USA, [3]Earth and Environmental Systems Institute, Pennsylvania State University, University Park, Pennsylvania, USA, [4]Department of Geological Sciences, University of Texas at El Paso, El Paso, Texas, USA, [5]Department of Ecosystem Science and Management, Pennsylvania State University, University Park, Pennsylvania, USA

Abstract Many surface soils are enriched in metals due to anthropogenic atmospheric inputs. To predict the persistence of these contaminants in soils, factors that impact rates of metal removal from soils into streams must be understood. Experiments at containerized seedling (mesocosm), pedon, and catchment scales were used to investigate the influence of vegetation on manganese (Mn) transport at the Susquehanna/Shale Hills Critical Zone Observatory (SSHCZO) in Pennsylvania, USA, where past atmospheric inputs from industrial sources have enriched Mn in surface soils. Large quantities of Mn that were leached from soil components into solution were taken up by vegetation; as a result, only relatively small quantities of Mn were removed from soil into effluent and streams. Manganese uptake into vegetation exceeded Mn losses in soil leachate by 20–200X at all scales, and net Mn loss from soils decreased in the presence of vegetation due to uptake into plant tissues. The majority of Mn taken up by forest vegetation at SSHCZO each year was returned to the soil in leaf litter and consequently immobilized as Mn oxides that formed during litter decomposition. Thus, plant uptake of Mn combined with rapid oxidation of Mn during litter decomposition contribute to long-term retention. Current release rates of soluble Mn from SSHCZO soils were similar to release rates from the larger Susquehanna River Basin, indicating that the processes observed at SSHCZO may be widespread across the region. Indeed, although atmospheric deposition of Mn has declined, surface soils at SSHCZO and throughout the eastern United States remain enriched in Mn. If recycling through vegetation can attenuate the removal of Mn from soils, as observed in this study, then Mn concentrations in soils and river waters will likely decrease slowly over time following watershed contamination. Understanding the role of vegetation in regulating metal transport is important for evaluating the long-term effects of historical and ongoing metal loading to soils.

1. Introduction

Over the geologically brief time scale of industrialization (decades to millennia), humans have redistributed elements across the Earth's surface, leading to enrichment of many elements in soils, water, air, and biota [*Nriagu and Pacyna*, 1988; *Rauch and Pacyna*, 2009; *Sen and Peucker-Ehrenbrink*, 2012]. Environmental regulation has curbed industrial emissions in many countries; however, soils and sediments act as a sink for deposition and provide a long-term record of atmospheric inputs [*Cole et al.*, 1990; *Ma et al.*, 2014]. Soils subsequently act as a source of atmospheric contaminants to river systems, even decades following deposition [*Rice et al.*, 2014]. The biogeochemical processes that regulate contaminant transport through watersheds remain unclear. To understand retention of contaminants in soils and removal into streams and rivers, it is necessary to identify the factors affecting their mobility and quantify rates of transfer between soils, water, and vegetation.

Manganese is one such contaminant that has been enriched in soils due to atmospheric inputs from industrial sources related to iron smelting, steel production, and coal combustion [*National Research Council*, 1973; *Nriagu and Pacyna*, 1988; *Cole et al.*, 1990; *Pacyna and Pacyna*, 2001]. While Mn enrichment in air and soils has been observed in the near vicinity of ferroalloy plants and roadways [*Lytle et al.*, 1995; *Boudissa et al.*, 2006; *Lucchini et al.*, 2007], Mn has only recently been discovered to contaminate soils over wider regions [*Herndon et al.*, 2011]. Consistent with broad geographic distribution of Mn deposition, it has been documented that fine Mn-rich particles or dissolved Mn in rain can disperse across great distances while

coarse Mn-bearing particles fall out of the atmosphere near their source [*Rahn and Lowenthal*, 1984; *Parekh*, 1990; *Buck et al*., 2010].

We previously reported on Mn contamination in soils at the Susquehanna Shale Hills Critical Zone Observatory (SSHCZO) located in the Susquehanna River Basin (SRB) in central Pennsylvania, USA [*Herndon et al*., 2011]. Mn enrichment in SSHCZO soils could not be explained by geologic inputs from mineral dust, and excess Mn was attributed to anthropogenic inputs from historical industrial sources such as local iron ore smelting and regional steel production and coal combustion [*Herndon et al*., 2011]. Although no monitoring was in place to document Mn deposition over the course of industrialization in central Pennsylvania (PA) (1800s to present), it is likely that Mn was deposited as either Mn oxide particles or dissolved in rain [*Lindberg and Harriss*, 1983; *Williams et al*., 1988; *U.S. Environmental Protection Agency*, 1984, 1985; *Nriagu and Pacyna*, 1988; *Pacyna and Pacyna*, 2001]. Declines in Mn concentrations in rivers near the Mn-impacted soils of central PA follow declines in atmospheric Mn deposition since the midtwentieth century, and we infer that the contaminant Mn is slowly being leached from soils into streams and rivers [*Herndon and Brantley*, 2011]. While Mn inputs to soils presumably derive from the point source nature of most Mn emitters, the rate of Mn loss from soils depends on the variability in ecosystem's capacities to retain Mn due to lithologic and biotic factors.

Plants can strongly impact element accumulation or release from soils, both enhancing mineral weathering over long time scales [*Drever*, 1994; *Bormann et al*., 1998; *Berner et al*., 2003; *Taylor et al*., 2009] and slowing the removal of elements from watersheds through biological uptake and storage on short time scales [*Johnson et al*., 1969; *Chaney et al*., 1997; *Balogh-Brunstad et al*., 2008]. For example, certain plant species can redistribute soil-derived Mn within a few decades, depleting Mn from mineral soil and enriching Mn in standing biomass and the organic horizon [*Jobbagy and Jackson*, 2004; *Li et al*., 2008]. Storage of Mn in the organic horizon can provide a pool of bioavailable Mn that can be reabsorbed by vegetation [*Shanley*, 1986], and annual fluxes of Mn through vegetation can exceed inputs to and outputs from watersheds [*Scudlark et al*., 2005; *Watmough et al*., 2007; *Navrátil et al*., 2007; *Landre et al*., 2010]. Indeed, high levels of foliar Mn (10–100 mmol kg^{-1}) have been reported in tree species throughout the northeastern United States, possibly contributing to the decline of Mn-sensitive sugar maple populations [*Horsley et al*., 2000; *St. Clair and Lynch*, 2005; *Kogelmann and Sharpe*, 2006]. While it is well known that vegetation can strongly impact the mobility of Mn under certain biotic and geochemical conditions, more studies are needed to quantify the impact of vegetation on regulating transport of Mn from soils into streams and rivers.

Here we quantified rates of Mn uptake into tree leaves and leaching from soils at the spatial scales of the containerized tree seedling (mesocosm), pedon, and catchment. Our overall objective was to evaluate the hypothesis that vegetation can slow the loss of Mn from soils into streams. In order to evaluate broader patterns of Mn redistribution in the environment, we used published geochemical data sets to examine Mn concentrations in the Susquehanna River and in soils of the United States [*U.S. Geological Survey*, 2014; *Smith et al*., 2013].

2. Methods

2.1. Mesoscale Experiment

For controlled mesocosm experiments, red oak seedlings were grown in soil pots in a greenhouse. Such mesocosm systems have previously been used to investigate plant influences on mineral weathering [*Andrews et al*., 2011b]. The soil pots contained mineral soil collected at the SSHCZO that was mixed with coarse sand (1:1) to facilitate aeration. The mineral soil was collected from the north slope of the SSHCZO in an area mapped as the Weikert soil series by *Lin et al*. [2006]. Surface soil (<10 cm) was discarded to remove the organic-rich surface layer from the mineral soil. Prior to the experiment, a sample of the soil medium (soil + coarse sand; <6% organic matter) was determined to contain 18 mmol kg^{-1} Mn after being fused with Li metaborate and analyzed on a Perkin-Elmer Optima 5300 inductively coupled plasma–atomic emission spectrophotometer (ICP-AES) at Pennsylvania State's Laboratory for the Isotopes and Metals in the Environment (LIME).

The study was conducted from May to August 2011 in a greenhouse in State College, PA, USA. The experiments were conducted in plastic tree pots (2.8 L, 10 × 10 × 36 cm; Stuewe and Sons, Inc., Corvallis, OR) filled with 3.2 kg

soil medium. Red oak seedlings (15–30 cm height; Cold Stream Farm, Freesoil, MI) were thoroughly rinsed to remove root-adhering soil and planted one per pot in moistened soil. The seedlings had buds upon delivery, and leaves began to emerge within 1 week. Plants were grown in a greenhouse with a temperature range of 20–30°C, and artificial lighting was supplied to ensure a photoperiod of 14 h. Drip lines delivered deionized (DI) water at a rate of 150–350 mL week^{-1} to each pot, which kept soils moist but well drained. Solute concentrations in influent water were below detection limits for ICP-AES for Al, Ca, Fe, Mg, and Mn (detection limit (DL) = 0.05 μg mL^{-1}) and K, Na, and P (DL = 0.10 μg mL^{-1}). After 4 weeks, pots were treated weekly with 10 mL nutrient (10 mmol L^{-1} monopotassium phosphate, 10 mmol L^{-1} calcium nitrate, and 1 mmol L^{-1} magnesium chloride; ~pH 4) and 5 mL 1 mmol L^{-1} potassium carbonate (pH 9.6) solutions prepared in ultrapure deionized water.

The experiment consisted of vegetated pots ($n = 12$) and nonvegetated pots ($n = 5$). Effluent water, defined as all water that drained from the bottom of the soil pot, was funneled into plastic tubing which dripped into 250 mL acid-washed amber-colored glass bottles. Effluent volume was recorded once per week over 16 weeks. Effluent subsamples were filtered (0.45 μm) and acidified with 2–3 drops ultrapure concentrated HNO_3. Solutions from 11 of the collection dates were analyzed on ICP-AES at Pennsylvania State University (PSU) LIME. In addition, a subset of samples with Mn concentrations below the ICP-AES detection limit (=0.09 μmol L^{-1}) was reanalyzed with inductively coupled plasma–mass spectrometry (ICP-MS). For the remaining 5 weeks where volume was recorded but effluent chemistry was not determined, solute concentrations were estimated as the average of concentrations from collection dates before and after.

Oak seedlings were harvested after 19 weeks of growth. Leaves were separated from the woody shoots, rinsed with DI water, and measured for leaf area with a LI-COR LI-3000A (±0.1 cm^2). Leaves were then dried at 60°C, weighed, ground in liquid nitrogen, and chemically analyzed on ICP-AES following dry ash and acid dissolution [*Miller*, 1998] at Pennsylvania State's Agricultural Analytical Services Laboratory.

Statistical analyses on mesocosm data were performed in Origin®. The mean and standard error of the mean were determined for each parameter. One-way analysis of variance was used to examine the influence of vegetation on log-transformed Mn concentrations in mesocosm effluent to a maximum significance level of $\alpha = 0.05$. *T* tests were used to determine whether slopes of best fit regression lines were significantly different from zero ($\alpha = 0.05$).

2.2. Field-Scale Study

2.2.1. Susquehanna Shale Hills Critical Zone Observatory

The SSHCZO is a 0.08 km^2 first-order catchment located in central PA nested within the larger Susquehanna River Basin. The catchment is characterized by planar hillslopes punctuated by relatively organic-rich swales that experience convergent water flow [*Lin et al*., 2006; *Andrews et al*., 2011a]. Soils that develop on the ridge are thin (<0.5 m) and well drained [*Lin et al*., 2006]. Soil pH is acidic and ranges from 4.0 ± 0.1 at the ridge to 4.7 ± 0.2 in the valley [*Jin et al*., 2011]. For all soils, soil organic carbon is highest near the soil surface (1–3 wt % SOC for 0–10 cm) and decreases with depth in the soil (<1 wt % SOC for >10 cm) [*Andrews et al*., 2011a]. Roots are found through the soil profile and are highly concentrated in the *O* and *A* horizons [*Lin et al*., 2006].

The SSHCZO catchment is underlain almost exclusively by the Silurian age Rose Hill shale formation that extends throughout the Appalachian region [*Jin et al*., 2011; *Dere et al*., 2013]. Manganese concentrations in the Rose Hill formation (14 mmol kg^{-1}) are similar to world averages for shale (≈15 mmol kg^{-1} [*Turekian and Wedepohl*, 1961]). No specific Mn minerals were documented above the detection limit of X-ray diffraction (a few weight percent) in the protolith or weathered soils [*Jin et al*., 2011; *Liermann et al*., 2011]; thus, Mn is most likely incorporated into primary clay minerals but can precipitate as poorly crystalline Mn oxides during rock weathering [*Herndon et al*., 2014].

Annual precipitation in the Shale Hills region is ~100 cm, and rainwater is acidic (pH = 4.5) due to industrial emissions throughout the region [*National Atmospheric Deposition Program*, 2011]. Daily discharge reported at the stream outlet averaged 113 ± 10 m^3 d^{-1} and ranged from 0 to 4160 m^3 d^{-1}, with zero flow occurring primarily in summer months and high flow following precipitation events in early spring and late fall (2008–2009 [*Duffy*, 2012]). Oak species (*Quercus rubra*, *Q. prinus* (i.e., *Q. montana*), and *Q. alba*) are the dominant catchment vegetation and comprise 63% of the total basal area [*Wubbels*, 2010]. Additional important genera include

hickory (*Carya tomentosa* and *C. glabra*; 13%), hemlock (*Tsuga canadensis*; 8%), pine (*Pinus virginiana* and *P. strobus*; 8%), and maple (*Acer saccharum* and *A. rubrum*; 5%). Litterfall peaks in October, and litter is comprised mostly of tree leaves with a smaller contribution (<14%) from fruits and woody debris [*Smith*, 2013].

The Shale Hills catchment has experienced several natural and anthropogenic perturbations during soil formation. First, the area shows evidence of freeze thaw and stratified slope deposits, consistent with a periglacial climate ~15 kyr [*Gardner et al*., 1991]. The SSHCZO, most likely logged extensively like the rest of central PA during colonial times, was recently harvested in the 1930s [*Wubbels*, 2010]. Finally, numerous ruins of furnaces are located within 30 km of the field site. Soils at the SSHCZO retain metals derived from the atmospheric deposition of particulates released to the atmosphere during iron smelting at these sites, as well as other byproducts of other industries [*Herndon et al*., 2011; *Ma et al*., 2014].

2.2.2. Field Sampling

Soil cores were collected from ridgetop ($n = 21$), midslope ($n = 6$), and valley positions ($n = 7$) (Figure S1 in the supporting information). Soil cores were excavated with a stainless steel auger from the mineral soil surface to the point of manual refusal, a physical approximation of the soil-bedrock interface [*Jin et al*., 2011]. At some sites, organic horizon samples ($n = 6$) were collected by hand from the soil surface prior to augering. Comprehensive geochemical data for these soil cores are reported in an online database [*Niu et al*., 2011].

Detailed methods of collection and chemical characterization for precipitation, stream, groundwater, and soil pore water samples have been previously described [*Andrews et al*., 2011a; *Jin et al*., 2011; *Herndon*, 2012]. Briefly, precipitation samples ($n = 61$) collected in 2002 were obtained from the National Atmospheric Deposition Program (NADP) for two sites (PA-15 and PA-42) located near the SSHCZO for trace element analysis. Major cation and anion concentrations are publically reported for these samples (nadp.sws.uiuc.edu). Stream water samples ($n = 345$) were collected into acid-washed plastic bottles at the catchment weir during 2008–2010. Groundwater samples ($n = 77$) were collected from 2.8 m depth by an ISCO autosampler installed near the catchment weir. Soil pore water samples ($n = 2403$) were collected between 2006 and 2011 from suction lysimeters installed at 10 to 20 cm depth increments at ridge, midslope, and valley floor (labeled as RT, MS, and VF) positions along south planar, south swale, north planar, and north swale hillslopes (labeled as SP, SS, NP, and NS) (Figure S1 in the supporting information).

Green leaves were collected from species representing >80% of surveyed trees in the SSHCZO [*Wubbels*, 2010; *Eissenstat et al*., 2013]. Upper canopy leaves were sampled from oak, hickory, and pine species multiple times from June to September 2009 and chestnut oak and sugar maple from June to September 2011 (Figure S1 in the supporting information). Leaves were obtained by rope climbing the trees and using a pole cutter to remove a section of the tree branch. Leaf litter was collected above the ground surface from 35 traps placed throughout the catchment in autumn 2011. Litter was collected once per week and weighed for total and species-specific mass [*Smith*, 2013]. Subsets of bulk leaf litter samples were retained for chemical analysis.

2.2.3. Chemical Analyses

To determine the total concentration of major elements in soils, representative air-dried bulk samples that included all rock fragments, sand, silt, and clay particles were ground to pass a 100 mesh sieve (<149 μm), fused with lithium metaborate at 950°C, and dissolved in 5% nitric acid. The resulting solutions were analyzed on ICP-AES at PSU LIME. Major element concentrations were accurate to ±3%, as determined for a diabase rock standard (U.S. Geological Survey (USGS) W-2). Pore water and filtered stream water samples were acidified with ultrapure concentrated nitric acid (HNO_3) and analyzed for cation concentrations on ICP-AES. For Mn concentrations below the detection limit for ICP-AES (DL = 0.09 μmol Mn L^{-1}), a value of one half the DL was used for calculations in this study. Samples for dissolved organic carbon analysis were filtered (0.45 μm), acidified with 2–3 drops of concentrated hydrochloric acid, and stored at 4°C until analysis on a Shimazdu TOC-5000A [*Andrews et al*., 2011a]. Precipitation samples acquired from NADP were acidified with ultrapure HNO_3 and analyzed on a quadrupole ICP–mass spectrometer (ICP-MS) at PSU LIME.

Dried green leaf and leaf litter samples were ground into powders in liquid nitrogen with a ceramic mortar and pestle. Powdered leaf samples (~150 mg) were fully digested with concentrated, ultrapure acids including nitric acid, hydrogen peroxide, and hydrofluoric acid (procedure adapted from *Hokura et al.* [2000]). Digest solutions were run by ICP-MS at Pennsylvania State using appropriate calibration curves. Method standards (National Institute of Standards and Technology 1547) and blanks were included in each sample set to assess potential contamination, bias, and efficiency of the acid digestion procedure.

2.3. Mass Balance Models

Mass balance models were used to quantify and compare Mn fluxes across mesocosm, pedon, and catchment scales. Each scale was modeled as a box that contained soil and experienced inputs and outputs of Mn: inputs to each box included precipitation and litterfall, and outputs from each box included plant uptake and loss in soil leachate. At the mesoscale, the box model included all soil contained within one mesocosm pot. At the pedon scale, the box model included all augerable mineral and organic soil for a unit land surface area (square meter) at the catchment ridge. At the catchment scale, the box model included all augerable soil within the Shale Hills catchment (0.08 km^2). Model equations were written with subscript j to refer to any mobile constituent of interest; however, in this discussion, j = Mn.

Manganese fluxes out of each soil box model included (i) plant uptake, the area-normalized rate that Mn was mobilized from the soil and transferred into aboveground biomass ($F_{j,veg}$; mmol m^{-2} yr^{-1}), and (ii) soil leachate, the area-normalized rate that Mn was leached from the soil and removed in effluent ($F_{j,eff}$; mmol m^{-2} yr^{-1}). At the field scales, all fluxes were integrated over 1 year. At the mesoscale, fluxes were measured over approximately 5 months and converted to units of mmol m^{-2} yr^{-1} for comparison to the field scales. This model included atmospheric input of Mn in precipitation at the field scales but assumed that current dry deposition was negligible, as reported for rural areas, and did not include the historically high values (i.e., >1 mmol m^{-2} yr^{-1}) that led to Mn enrichment in these soils [*Herndon et al.*, 2011].

Given that fluxes are not directly comparable from mesoscale to field scale due to the artificial constraint on land surface area in the mesocosm pots, $F_{j,veg}$ and $F_{j,eff}$ were normalized to the mass of Mn contained in the soil per unit land surface area ($M_{j,w}$; mmol m^{-2}):

$$k_{j,veg} = F_{j,veg}/M_{j,w} = f_{i,veg}/t \quad (1)$$

$$k_{j,eff} = F_{j,eff}/M_{j,w} = f_{i,eff}/t \quad (2)$$

Here k values describe the fraction of Mn removed from soil (f_j) per unit time (t) and either transferred into foliage ($k_{j,veg}$; yr^{-1}) or leached from the soil into effluent ($k_{j,eff}$; yr^{-1}), equivalent to first-order rate constants calculated for box models of environmental systems [*Lerman and Wu*, 2008].

At the mesoscale, effluent fluxes and rate constants were separately determined for vegetated pots (superscript "*v*") and nonvegetated pots (superscript "*n*"). The pedon and catchment-scale systems are inherently vegetated. The following sections summarize the results of the mass balance model calculations obtained for mesocosm, pedon, and catchment scales using the chemical data reported for soil, water, and vegetation samples. Details of flux calculations at each scale are provided in the supporting information.

2.4. Geochemical Databases

Element concentrations in soils from across the conterminous United States (n = 4859) were recently reported in an extensive geochemical survey [*Smith et al.*, 2013]. Enrichment and depletion of Mn in the surface soils relative to deeper soils were examined in this study using the mass transfer coefficient $\tau_{i,j}$ [*Brimhall and Dietrich*, 1987; *Anderson et al.*, 2002]:

$$\tau_{i,j} = \frac{C_{j,w}C_{i,p}}{C_{j,p}C_{i,w}} - 1 \quad (3)$$

The $\tau_{i,j}$ values indicate enrichment ($\tau_{i,j} > 0$) or depletion ($\tau_{i,j} < 0$) of a mobile element j (=Mn) in weathered surface soil (subscript w) relative to the parent material (subscript p) by normalizing concentrations to an immobile element i (=Ti). A mobile element that is chemically weathered and removed from a soil will exhibit depletion, whereas an element that is added to a soil from external inputs (e.g., atmospheric deposition) or translocated due to biological processing (e.g., nutrient-like recycling) will exhibit enrichment at the soil surface [*Brantley and Lebedeva*, 2011]. At SSHCZO, the magnitude of Mn enrichment in soils cannot be explained by biological uplift alone, and mass balance requires external input from atmospheric deposition [*Herndon et al.*, 2011; *Kraepiel et al.*, 2015]. Here the composition of surface soil (0–5 cm depth) was examined relative to the parent *C* horizon (variable depth ranges) at each site.

Water quality data for the Susquehanna River were obtained from the National Water Information System provided by the U.S. Geological Survey [*U.S. Geological Survey*, 2014]. Concentrations of dissolved Mn in river

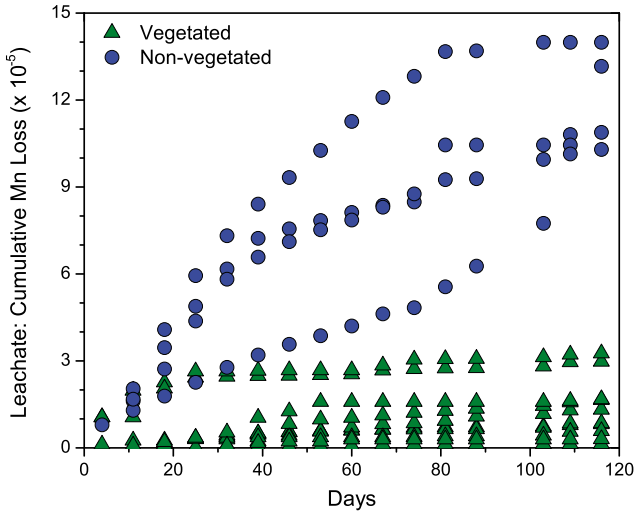

Figure 1. The cumulative fraction of Mn loss in effluent ($f_{Mn,eff}$; unitless) from mineral soil is plotted versus time for pots with seedlings (green triangles) and without seedlings (blue circles). The rate constant describing Mn loss in effluent ($k_{Mn,eff}$) was calculated from the slope of the line for each pot (equation (2)).

water ($C_{Mn,river}$; μmol L^{-1}) were collated for all sites along each river. We further examined three sites along the main branch of the Susquehanna River for which reported discharge (Q) and $C_{Mn,river}$ data spanned a wide range of dates: Danville, PA (site 01540500; $Q = 440 \pm 10\ m^3\ s^{-1}$; 85 $C_{Mn,river}$ values from 1972 to 1995); Harrisburg, PA (site 01570500; $Q = 997 \pm 19\ m^3\ s^{-1}$; 186 $C_{Mn,river}$ values from 1970 to 1995); and Conowingo, MD (site 01578310; $Q = 1170 \pm 47\ m^3\ s^{-1}$; 283 $C_{Mn,river}$ values from 1978 to 2010). Drainage areas (A_{SRB}; m^2) have been reported for Danville (=$2.91 \times 10^{10}\ m^2$), Harrisburg (=$6.24 \times 10^{10}\ m^2$), and Conowingo (=$7.02 \times 10^{10}\ m^2$) [*U.S. Geological Survey*, 2012].

3. Results

3.1. Mesocosm Geochemistry and Mass Balance Model

Mesocosm experiments were used to test the hypothesis that vegetation slows the loss of Mn from soil into leachate. Indeed, the average concentration of Mn in effluent draining from the mesocosms ($C_{Mn,eff}$; μmol) was significantly higher in nonvegetated (2.8 ± 0.6 μmol L^{-1}) than vegetated (0.72 ± 0.10 μmol L^{-1}) systems ($p < 0.001$) (Table S2 in the supporting information). Effluent volume was also higher from nonvegetated pots since no water was lost to transpiration, yielding greater fluxes of Mn to effluent: $F^n_{Mn,eff} = 1.4 \pm 0.3\ mmol\ m^{-2}\ yr^{-1} > F^v_{Mn,eff} = 0.23 \pm 0.06\ mmol\ m^{-2}\ yr^{-1}$. Here Mn losses to effluent were measured weekly over 5 months, and fluxes were converted to units of mmol $m^{-2}\ yr^{-1}$ for comparison to the field scales. This conversion assumes that fluxes are constant over 1 year since we could not evaluate seasonality in the greenhouse. The cumulative fraction of soil Mn leached into effluent ($f_{Mn,eff}$; unitless) increased over time more rapidly in the nonvegetated than vegetated pots (Figure 1). As a result, the fraction leached during the experiment in nonvegetated pots, $k^n_{Mn,eff}$ (=$32 \pm 3 \times 10^{-5}\ yr^{-1}$), was 10X higher than in vegetated pots, $k^v_{Mn,eff}$ (=$3.2 \pm 0.7 \times 10^{-5}\ yr^{-1}$) ($p < 0.001$) (equation (2) and Table 1).

At harvest, Mn concentrations in the foliage ($C_{Mn,fol} = 79.9 \pm 5.1$ mmol kg^{-1}) exceeded "excessive" levels (>7 mmol kg^{-1} [*Kabata-Pendias and Pendias*, 2001]) (Table S1 in the supporting information). The rate that Mn was mobilized from the mineral soil and taken up into vegetation, $F_{Mn,veg}$ (=34.3 ± 4.0 mmol $m^{-2}\ yr^{-1}$), was calculated as the mass of Mn in foliage at harvest normalized to mesocosm surface area and growth period and expressed in units of mmol $m^{-2}\ yr^{-1}$. The fraction of soil Mn taken up into foliage,

Table 1. Average Parameters (±Standard Error) Reported for Mesoscale and Field Scale

	Fluxes (mmol $m^{-2}\ y^{r-1}$)		Rate Constants ($\times 10^{-5}\ yr^{-1}$)	
	$F_{Mn,eff}$	$F_{Mn,veg}$	$k_{Mn,eff}$	$k_{Mn,veg}$
Mesocosm: vegetated[a]	0.14 ± 0.02	34.3 ± 4.0	3.2 ± 0.7	630 ± 70
Mesocosm: nonvegetated[a]	0.88 ± 0.20	0	32 ± 3	0
SSHCZO: ridge pedon	0.66 ± 0.15	18 ± 4	2.8 ± 0.7	75 ± 21
SSHCZO: catchment	0.33 ± 0.02	18 ± 4	1.7 ± 0.5	93 ± 27
Susquehanna River Basin (2000–2010)	not applicable (NA)	NA	1.8 ± 0.9	NA

[a]Fluxes and rate constants for mesocosms were calculated for 19 week experiments and are expressed here in units of mmol $m^{-2}\ yr^{-1}$ and yr^{-1}.

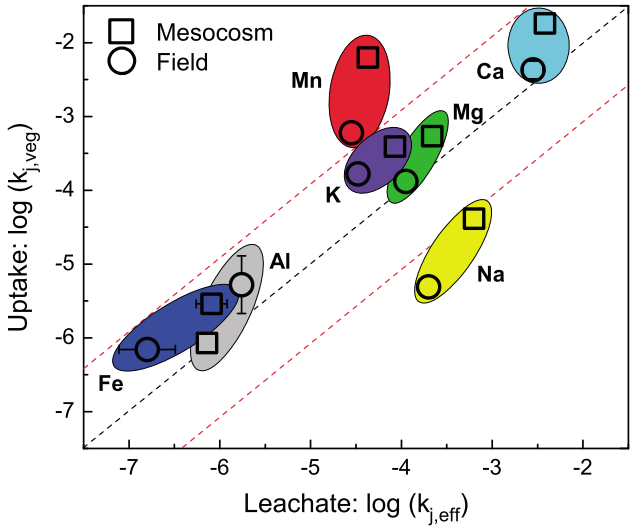

Figure 2. Log-log plot of the annual fraction of Mn removed from soil and either transferred into foliage ($k_{j,veg}$; $\times 10^{-5}$ yr^{-1}) or leached from the soil into effluent ($k_{j,eff}$; $\times 10^{-5}$ yr^{-1}) as measured at the scales of the vegetated mesocosm (squares) and ridge pedon (circles). Uptake and leaching fluxes in the mesocosms were measured over 19 weeks and converted to units of yr^{-1} by assuming fluxes remained constant during the year. The black dashed line indicates $k_{j,veg} = k_{j,eff}$, and the red dashed lines indicate order of magnitude deviation from the black line (e.g., $k_{j,veg} = 10 \times k_{j,eff}$ and $k_{j,eff} = 10 \times k_{j,eff}$).

$k_{Mn,veg} = 627 \pm 71 \times 10^{-5}$ yr^{-1} (equation (3)), was ~200X greater than the fraction lost to leaching during the experiment ($k^{v}_{Mn,eff} = 3.2 \pm 0.7 \times 10^{-5}$ yr^{-1}) (Table 1). Fluxes were converted to units of mmol m^{-2} yr^{-1} for comparison to the field scales. This conversion assumes that uptake rates measured over 5 months in the greenhouse are constant over 1 year. However, these uptake rates represent maximum estimates since Mn uptake is seasonal in temperate forests. For comparison, given that the growth period for seedlings (19 weeks) was similar to the growing season at Shale Hills (leaf out in mid-April to maximum foliar Mn in late August), the mass of Mn transferred into foliage during the experiment may approximately equal the annual uptake, yielding a minimum estimated value of $k_{Mn,veg} = 210 \pm 24 \times 10^{-5}$ yr^{-1}.

In order to explore how the seedlings cycled Mn relative to other elements, we compared uptake into foliage ($k_{j,veg}$; equation (1)) and leaching into effluent ($k_{j,eff}$; equation (2)) for a suite of elements (j = K, Mg, Na, Ca, Mn, Fe, and Al). Manganese uptake far exceeded leaching ($k_{Mn,veg}/k_{Mn,eff} > 100$) and was higher than for the major plant nutrients, K, Mg, and Ca, for which $k_{j,veg}/k_{j,eff} < 10$ (Figure 2). Micronutrient Fe was also preferentially taken up, while the nonessential element Na was lost to leaching ($k_{Na,veg}/k_{Na,eff} < 1$) because it was taken up in relatively small quantities.

For all elements, leaching from nonvegetated pots exceeded leaching from vegetated pots during the experiment (Table 2). This was due in part to transpiration, which reduced average effluent volume by ~50% in vegetated pots; however, the transpiration effect can only explain differences for Na, which was reduced by 50% in the vegetated pots, similar to the reduction in effluent volume. In contrast, leaching of

Table 2. Uptake ($k_{j,veg}$; Equation (1)) and Leaching ($k_{j,eff}$; Equation (2)) for Elements at Mesoscale and Pedon Scale ($\times 10^{-5}$ yr^{-1})

	Ca	K	Mg	Mn	Al	Fe	Na
			Mesocosms[a]				
$k^{v}_{j,eff}$	383	8.6	22	3.2	0.07	0.08	63
Standard error	57	1.3	3	0.7	0.02	0.03	8
$k_{j,veg}$	1830	39	54	627	0.09	0.29	4.1
Standard error	260	4	7	71	0.02	0.07	0.6
$k^{v}_{j,eff} + k_{j,veg}$	2390	52	81	692	0.16	0.40	68
Standard error	350	5	11	79	0.04	0.11	9
$k^{n}_{j,eff}$	1640	64	76	32	0.54	0.50	141
Standard error	410	12	20	3	0.24	0.34	37
			Pedon scale				
$k^{v}_{j,eff}$	427	16.5	13.2	59.8	0.52	0.07	0.49
Standard error	118	2.2	1.8	11.1	0.47	0.01	0.13
$k_{j,veg}$	281	3.3	11.2	2.8	0.17	0.02	20.1
Standard error	69	0.3	0.7	0.7	0.01	0.01	2.4

[a]The $k_{j,veg}$ and $k_{j,eff}$ for mesocosms were calculated in 19 week experiments and are expressed here in units of yr^{-1}.

Mn, K, Ca, Mg, Al, and Fe from nonvegetated pots exceeded leaching from vegetated pots by 3–10X due to uptake into plant tissue (Table 2). Although less Mn was leached in the presence of vegetation, total mobilization ($k_{Mn,veg} + k_{Mn,eff}$) increased (Table 2). Calcium also showed a trend of increased mobilization but decreased leaching in vegetated pots. In contrast, for all other elements, total mobilization in vegetated systems was less than or approximately equal to that in nonvegetated systems.

3.2. Pedon and Catchment-Scale Geochemistry

The depth-weighted average Mn concentrations in weathered soils ($C_{Mn,w}$; mmol kg^{-1}) collected from all depths at the SSHCZO were high in ridge (=41 ± 4 mmol kg^{-1}, n = 120), midslope (=24 ± 3 mmol kg^{-1}, n = 46), and valley soils (=22 ± 2 mmol kg^{-1}, n = 91) relative to the parent shale ($C_{Mn,p}$ = 15 ± 2 mmol kg^{-1}) (Table S1 in the supporting information). Manganese concentrations were especially high in the organic horizon ($C_{Mn,org}$ = 117 ± 64 mmol kg^{-1}) and in the upper mineral soils and decreased with depth (Figure 3a and Table S1 in the supporting information). As detailed in the supporting information, the area-normalized mass of Mn contained within soil ($M_{Mn,w}$) averaged 23,900 ± 6500 mmol m^{-2} for ridge soils and 19,400 ± 2500 mmol m^{-2} in soils across the entire catchment.

Manganese concentrations in soil pore waters ($C_{Mn,pw}$; μmol L^{-1}) were highest near the soil surface and decreased toward bedrock (Figure 3b), similar to reported trends for exchangeable Mn (ranges from 0.18 to 3.4 mmol kg^{-1}) [*Jin et al.*, 2010]. Additionally, $C_{Mn,pw}$ values were higher in swale than planar soils (Figure 3b): averaged over all depths, the south planar ridgetop (SPRT = 1.45 ± 0.36 μmol L^{-1}), midslope (SPMS = 0.68 ± 0.08 μmol L^{-1}), and valley floor (SPVF = 0.42 ± 0.04 μmol L^{-1}) pore waters were lower than the south swale ridgetop (SSRT = 8.67 ± 0.73 μmol L^{-1}), midslope (SSMS = 1.41 ± 0.13 μmol L^{-1}), and valley floor (SSVF = 0.59 ± 0.15 μmol L^{-1}) pore waters. In the swale pore waters, Mn concentrations increased exponentially as a function of dissolved organic carbon (DOC) (Figure S2 in the supporting information). In comparison, no correlation between Mn and DOC was observed for pore waters in planar soils. As argued by *Andrews* [2011], swales may act as sources of DOC and metal (Mn, Fe, and Al) transport into stream waters.

In the stream at the catchment outlet, Mn concentrations ($C_{Mn,stream}$; μmol L^{-1}) were negatively correlated with stream discharge (Q; m^3 d^{-1}) and were generally high during summer months when streamflow was minimal and lower during spring and fall when streamflow was high (Figure 3b). Pulses of high Mn concentrations observed in summer may document periodic flushing of Mn-rich water into the stream from decomposing plant matter in swales [*Andrews*, 2011]. For comparison, stream concentrations of Na, released by plagioclase dissolution and not taken up by plants as a nutrient, remained relatively constant (33.5 ± 0.5 μmol L^{-1}) relative to Mn (4.2 ± 0.6 μmol L^{-1}) over a range of 6 orders of magnitude in discharge (Figure 3b). Manganese concentrations in groundwater collected near the stream weir (=0.047 ± 0.002 μmol L^{-1}) and in precipitation ($C_{Mn,ppt}$ = 0.045 ± 0.006 μmol L^{-1}) were low relative to stream and pore waters (Table S1 in the supporting information).

Green leaves collected in late summer had higher foliar Mn concentrations ($C_{Mn,fol}$; mmol kg^{-1}) than leaves collected in early summer (Table S1 in the supporting information). Following previous studies, $C_{Mn,fol}$ values from late summer were used as best approximations of maximum foliar Mn concentrations [*McCain and Markley*, 1989]. Of the major tree species, hickories exhibited the highest late summer concentrations of foliar Mn (68.3 ± 4.5 mmol kg^{-1}), followed by sugar maples (48.6 ± 4.0) and oaks (42.8 ± 3.7), then pines (17.3 ± 1.3). Manganese concentrations in leaf litter increased from late August (=33.0 ± 3.1 mmol kg^{-1}) to early October (=52.2 ± 3.8) to late October (59.0 ± 4.6) (Table S3 in the supporting information). The rate of litterfall (g m^{-2} week^{-1}) peaked in late October, concurrent with maximum concentrations of Mn.

3.2.1. Pedon and Catchment-Scale Mass Balance Models

Mass balance models were used to calculate Mn uptake into vegetation and loss from soils into leachate at the pedon and catchment scales. The net flux of Mn chemically weathered and removed from the ridge pedon ($F_{Mn,eff}$ = 0.66 ± 0.15 mmol m^{-2} yr^{-1}) was calculated as the output solute flux (=0.71 mmol m^{-2} yr^{-1}) minus the influent precipitation (=0.045 mmol m^{-2} yr^{-1}). The output solute flux was calculated as the product of $C_{Mn,pw}$ at the soil-bedrock interface (=1.4 ± 0.3 μmol L^{-1}) and the volume of water that flushes the soil each year (=520 L m^{-2} yr^{-1}). To understand this Mn loss, $F_{Mn,eff}$ was normalized to the mass of Mn stored in ridge pedons (equation (1)); thus, Mn lost in effluent from ridge soils was best described by $k_{Mn,eff} = 2.8 \pm 0.7 \times 10^{-5}$ yr^{-1}.

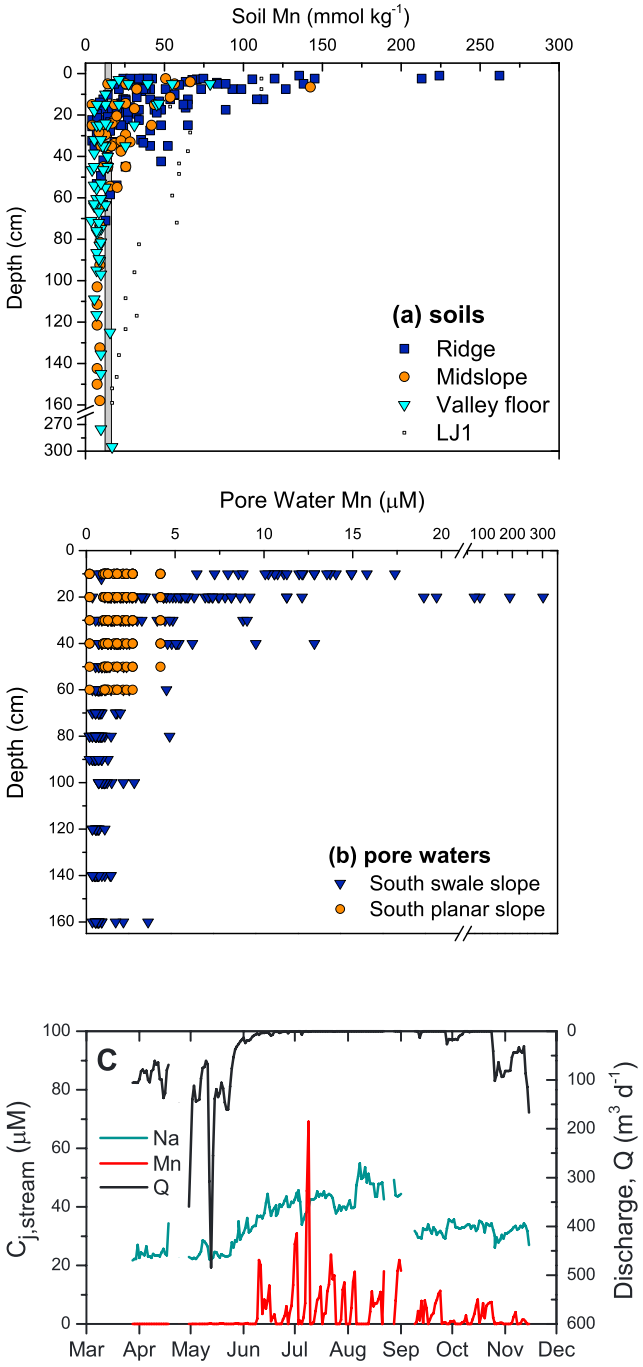

Figure 3. Manganese concentrations in (a) bulk soil ($C_{Mn,w}$; mmol kg^{-1}) versus depth for soil samples collected from ridge, midslope, and valley sites in the SSHCZO catchment (Figure S1 in the supporting information). The Mn concentration in bedrock is shown as a vertical shaded bar. (b) Mn concentrations in pore waters (μmol L^{-1}) decrease with depth and are lower in soils on the planar than the swale hillslope. (c) Seasonal variability in Mn and Na concentrations plotted with average daily discharge for 2008. Note that discharge values increase from the top axis down.

At the catchment scale, the net loss of dissolved Mn from the catchment ($F_{Mn,eff} = 0.33 \pm 0.02$ mmol m^{-2} yr^{-1}) was calculated as the annual dissolved load in the stream minus inputs from precipitation. Dissolved load was calculated with the USGS program LOADEST by fitting models to concurrent measurements of concentration-discharge data [*Runkel et al.*, 2004]. Normalizing $F_{Mn,eff}$ to $M_{Mn,w}$ averaged across all catchment soils (=19,400 ± 2500 mmol m^{-2}) yielded $k_{Mn,eff} = 1.7 \pm 0.5 \times 10^{-5}$ yr^{-1} at the catchment scale, which was within error of $k_{Mn,eff}$ at the mesocosm and pedon scales (Table 1). From this result, we infer that current Mn loss at the catchment scale was consistent with Mn loss from vegetated mineral soils as observed at the mesocosm and pedon scales. However, pulses of high Mn concentrations in stream water were excluded from LOADEST in order for the model to converge, and catchment-scale Mn losses may be underestimated due to elimination of these values.

Each year, dissolved Mn is transferred from soil into vegetation during the growing season and stored in woody biomass and foliage. For this mostly deciduous forest, Mn contained in foliage is returned to the soil each year in either litterfall or throughfall. Plant uptake (=annual storage in woody and foliar tissue) and litterfall (leaves + woody debris) were calculated to investigate rates of Mn transfer through vegetation relative to rates of Mn loss from soil in leachate. These fluxes were assumed to be approximately equal across pedon and catchment scales. Throughfall, which may account for ~20–40% of Mn loss from foliage [*Bergkvist and Folkeson*, 1995; *Navrátil et al.*, 2007; *Watmough et al.*, 2007; *Landre et al.*, 2010], was not collected for this study; therefore, uptake and litterfall fluxes represent minimum estimates.

Mn uptake into vegetation ($F_{Mn,veg} = 18 \pm 4$ mmol m^{-2} yr^{-1}) was 10–100X greater than both Mn inputs in precipitation and Mn losses in leachate (Figure 4). The flux of Mn from soil into foliage ($F_{Mn,fol} = 15 \pm 4$ mmol m^{-2} yr^{-1}) represented >85% of total uptake and was large relative to annual storage

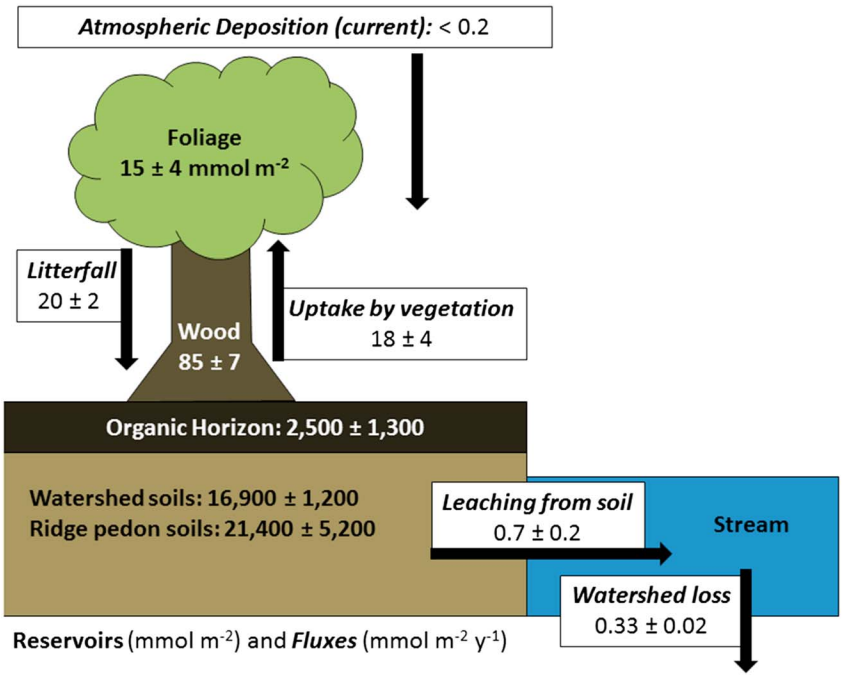

Figure 4. Reservoirs (mmol m^{-2}) and fluxes (mmol m^{-2} yr^{-1}) of manganese in the SSHCZO catchment.

in woody tissue ($F_{Mn,wood} = 2.5$ mmol m^{-2} yr^{-1}). The flux of Mn returned to the soil from vegetation each year as litterfall ($F_{Mn,litter} = 20.3 \pm 1.6$ mmol m^{-2} yr^{-1}) was within error of $F_{Mn,fol}$ (Table 2). Although the total mass of Mn contained in foliage (=15 mmol m^{-2}) and woody biomass (=85 mmol m^{-2}) represented <1% of the total Mn contained in catchment soils, fluxes of Mn into and out of vegetation were orders of magnitude greater than net inputs and outputs from the soil (Figure 4). Similar to $F_{Mn,eff}$, $F_{Mn,veg}$ was modeled as first order with respect to $M_{Mn,w}$ to derive $k_{Mn,veg}$ at pedon (=$75 \pm 21 \times 10^{-5}$ yr^{-1}) and catchment (=$93 \pm 27 \times 10^{-5}$ yr^{-1}) scales (equation (1)). These values indicate that ~50X more Mn was mobilized and taken up by vegetation than was leached from the soil.

In order to explore how the forest vegetation cycled Mn relative to other elements, we calculated uptake ($k_{j,veg}$; equation (1)) and leaching ($k_{j,eff}$; equation (2)) for a suite of elements (j = Mn, Fe, Al, K, Mg, Na, and Ca) at the pedon scale. The fraction of Mn taken up into foliage exceeded the fraction of Mn lost in leachate by over an order of magnitude ($k_{Mn,veg}/k_{Mn,eff} > 10$; Figure 2). In comparison, uptake only slightly exceed leaching for major plant nutrients K, Mg, and Ca ($k_{j,veg}/k_{j,eff} < 10$), while Na was preferentially lost to leaching ($k_{Na,veg}/k_{Na,eff} < 1$). For these calculations, uptake comprised the mass of each element transferred into foliage per unit land surface area per year, and leaching comprised the mass of each element chemically weathered and removed from a ridge pedon in soil pore water per year. For all elements, uptake and leaching were similar at the mesoscale and field scale although slightly higher for the mesocosm systems. As discussed in section 3.1, uptake in the mesocosm systems may be overestimated by ~3X due to the assumption that uptake rates measured over 19 weeks remain constant over 1 year.

3.3. Database Soil and Water Geochemistry

Soils exhibiting Mn enrichment were concentrated in the eastern United States (Figure 5). Manganese was enriched in 22% of surface soils in the United States by at least a factor of 2 relative to *C* horizons ($\tau_{Ti,Mn} \geq 1$). In contrast, the majority of examined soils across the country (~75%) exhibited only moderate Mn enrichment or depletion ($\tau_{Ti,Mn} = -0.5$–1), while fewer were mostly depleted of Mn ($\tau_{Ti,Mn} < -0.5$). The broad distribution of Mn enrichment identified here is consistent with similar patterns observed previously using a lower-resolution data set ($n = 455$ soils) and may be attributed at least in part to atmospheric deposition from industrial sources [*Herndon et al.*, 2011; *Herndon and Brantley*, 2011]. Five elements in addition to Mn (Hg, Cd, Pb, P, and S) exhibited positive median $\tau_{Ti,j}$ values in surface soils (Figure S3 in the

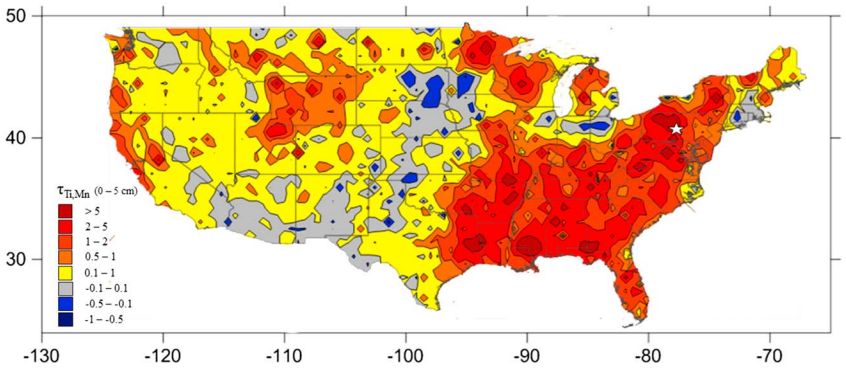

Figure 5. Color contour map of $\tau_{Ti,Mn}$ values for surface soils (0–5 cm) of the conterminous United States. Soils in the eastern United States are enriched in Mn relative to their *C* horizons (warm colors: $\tau_{Ti,Mn} > 0.1$), while other soils are depleted (cool colors: $\tau_{Ti,Mn} < -0.1$) or show minimal enrichment or depletion (grey: $-0.1 < \tau_{Ti,Mn} < 0.1$). Surface enrichment is indicative of atmospheric deposition and/or biological recycling processes, while depletion indicates chemical weathering. Contours were generated using inverse distance weighting function. The location of the Susquehanna Shale Hills Critical Zone Observatory is indicated by the white star.

supporting information). Although it is not feasible to attribute a single process to all locations without detailed site investigation, our studies indicate that both atmospheric deposition and biological recycling can contribute to Mn enrichment in surface soils. The observed patterns of Mn enrichment indicate that one or both of these processes are important in soils throughout the eastern United States.

Records of water chemistry along the Susquehanna River were examined to put the observations of Mn mobilization at the mesocosm, pedon, and catchment scales into a larger context. Manganese concentrations in river water ($C_{Mn,river}$; $\mu mol\,L^{-1}$) along the Susquehanna River decreased by a factor of 10 from the first measurements in 1957 to the most recently reported data in 2010 ($p < 0.001$) (Figure S4 in the supporting information). To estimate the current rate of Mn removal from soils in the Susquehanna River Basin, we expand equation (2) to calculate $k_{Mn,eff}$ for the drainage area of each Susquehanna River site (Danville, Harrisburg, and Conowingo) for the most recent decade (2001–2010):

$$k_{j,\mathrm{eff}} = \frac{F_{j,\mathrm{eff}}}{M_{j,w}} = \frac{C_{j,\mathrm{river}} Q}{A_{\mathrm{SRB}} C_{j,w} d \rho_w} \tag{4}$$

Here Q is the discharge ($m^3\,yr^{-1}$) and A_{SRB} is the drainage area (m^2) for each site. $C_{Mn,river}$ ($=0.78 \pm 0.12\ \mu mol\,L^{-1}$) was averaged over all sites ($n = 50$). For simplicity, we used a soil bulk density value $\rho_w = 1520\ kg\,m^{-3}$ (similar to measurements at Shale Hills) and an average depth of soil $d = 1$ m. We used a value for $C_{Mn,w}$ ($=14.7 \pm 1.1\ mmol\,kg^{-1}$) averaged over all depths in 360 soil samples from 65 soil cores developed on various lithologies throughout Pennsylvania [*Ciolkosz and Amistadi*, 1993; *Ciolkosz et al.*, 1998; *Ciolkosz*, 2000].

Manganese losses from the SRB to the Susquehanna River were approximately equal at all sites ($k_{Mn,eff} = 1.8 \pm 0.9 \times 10^{-5}\ yr^{-1}$) and within error of current $k_{Mn,eff}$ values calculated for the SSHCZO (Table 1). Based on these values and historical Mn concentrations, we estimated that the total dissolved Mn mass carried out by the river at each of the three locations over the 53 year period comprised <1% of total soil Mn in the drainage basin. In other words, the total loss of Mn from the basin was small compared to the total Mn mass in the soil.

4. Discussion

Surface soils throughout the eastern United States are enriched in Mn relative to deeper soil horizons. The observed enrichment may be attributed, as least in part, to atmospheric inputs from industrial sources which persist in surface soils even though atmospheric deposition of Mn has declined over the past few decades [*Herndon et al.*, 2011]. As observed in this study, large quantities of Mn that are leached from atmospheric inputs and soil components (minerals + decomposing organic matter) each year are taken up by forest vegetation and stored in leaves; as a result, only relatively small quantities of Mn are released to the stream. Although Mn has a short residence time in leaves, it has a longer residence time in the Mn

oxides that form during litter decomposition. If vegetation can attenuate the removal of Mn from soils, then concentrations in soils and river waters may decrease slowly over time following soil contamination. Thus, in industrialized areas such as the Ohio-Pennsylvania-West Virginia corridor, where Mn has been emitted to the atmosphere from point locations since the late 1700s and deposited to soils, we infer that recycling through vegetation slows the removal of atmospherically deposited Mn from impacted watersheds. Retention of atmospheric contaminants in ecosystems has also been documented for other elements (Hg, S, and Pb) demonstrating widespread enrichment in surface soils [e.g., *Selin*, 2009; *Filippelli and Laidlaw*, 2010; *Rice et al*., 2014].

Containerized seedling experiments were used to directly quantify the impact of vegetation on fluxes of Mn leached from soil and lost into effluent water. We observed that vegetation drastically slowed Mn loss into soil leachate by removing Mn from the soil and storing it in leaves during the experiment. Manganese losses to effluent decreased in pots with tree seedlings, and uptake of Mn by seedlings exceeded losses in effluent by 2 orders of magnitude. To evaluate whether attenuation of losses by vegetation was unique to Mn, we quantified uptake and leaching for a suite of major rock-derived cations (Figure 2). Since Mn is a micronutrient for plants, it is not expected to be taken up in large quantities; yet the ratio of uptake to leaching was higher for Mn (~200X) than for major plant nutrients (Ca, Mg, and K) and metal cations (Fe and Al) (<5X). In contrast, the nonnutrient Na did not accumulate in plant tissue and was preferentially leached to soil solution.

Pedon and watershed-scale studies at the SSHCZO were used to evaluate Mn cycling in temperate forest ecosystems. Uptake of Mn into forest vegetation exceeded losses in soil leachate by ~20X more than for other major cations (<5X). Given these observations, we conclude that vegetation exerts a stronger influence on the cycling of Mn than other major cations in ecosystems similar to the SSHCZO. The capacity of plants to accumulate Mn far in excess of nutritional requirements may contribute to ecosystem toxicity in catchments throughout the northeastern U.S. where Mn is readily soluble [e.g., *Kogelmann and Sharpe*, 2006; *St. Clair and Lynch*, 2005].

While a portion of Mn that is taken up from soil into forest vegetation is stored for decades in standing biomass, the majority is returned to the soil each year in litterfall (Figure 4). Dissolved Mn that is released from leaf and woody litter during decomposition is subsequently (1) bound to exchange sites on minerals and organic matter in the soil [*Shanley*, 1986; *Jin et al*., 2011], (2) immobilized as Mn oxides during litter decomposition [*Herndon et al*., 2014], or (3) leached from soils into streams. We previously determined that soil Mn at SSHCZO is primarily contained in Mn oxides that form during litter decomposition and shale weathering [*Herndon et al*., 2014]. Here we determine that Mn released into pore waters from decomposition and mineral dissolution is taken up by vegetation in large quantities that exceed losses from soils to streams. Dissolved Mn concentrations are high near the soil surface but decrease with depth (Figure 3b), and little Mn is leached from the soil profile. Consequently, uptake of Mn by certain plant species combined with rapid oxidation of Mn during litter decomposition may concentrate Mn near the soil surface and contribute to long-term retention. However, as observed at the SSHCZO, organic-rich soils in the swales may serve as a source of Mn transport into the stream during periods of decomposition and flushing with rainwater. Pulses of high Mn exiting the catchment in the stream, which were not captured by our calculations of dissolved loads, could reduce the average residence of Mn in the catchment (Figure 3c).

By integrating mass balance models from the tree pot to the watershed, we establish that Mn uptake into vegetation and leaching from soils are consistent across widely different spatial scales. In particular, uptake exceeds leaching by >10X in both mesocosm and field studies, and the annual fraction of Mn lost from soils into leachate ($k_{Mn,eff}$) is approximately equal at the scales of the vegetated mesocosm ($3.2 \pm 0.7 \times 10^{-5}\,yr^{-1}$), ridge pedon ($2.8 \pm 0.7 \times 10^{-5}\,yr^{-1}$), SSHCZO watershed ($1.7 \pm 0.5 \times 10^{-5}\,yr^{-1}$), and Susquehanna River Basin ($1.8 \pm 0.9 \times 10^{-5}\,yr^{-1}$). We infer from our experiments that processes associated with recycling through vegetation actively sequester Mn throughout the SRB, similar to the SSHCZO; otherwise, leaching of Mn from SRB soils would be higher. Thus, uptake of Mn by vegetation and storage in Mn oxides formed during litter decomposition may control the transport of Mn through watersheds and delivery to river systems across broad regions.

5. Conclusions

This study demonstrates that vegetation plays an important role in controlling the retention of Mn in temperate watersheds. Specifically, we determine that certain types of vegetation, such as the temperate

forest studied here, have the ability to slow the rate that Mn is transferred from soils into water systems. Large quantities of Mn that are leached from soil components (e.g., soil minerals + decomposing organic matter) into solution are taken up by vegetation: as a result, only relatively small quantities of Mn are lost from soils into effluent. Much if not most of the Mn that is taken up by forest vegetation is retained for years in biomass or in Mn oxides that form during litter decomposition [*Herndon et al*., 2014]. We also conclude that Mn is broadly enriched in surface soils of the eastern United States, similar to the SSHCZO, indicating that forest retention of atmospheric Mn inputs may be prevalent in contaminated ecosystems. Future work should examine the relative roles of long-lived biomass versus decomposition products (e.g., Mn oxides) for their potential to store Mn and control how long excess Mn can persist in ecosystems.

Acknowledgments

The data for this paper are available through the Susquehanna/Shale Hills Critical Zone Observatory (SSHCZO) data set (www.criticalzone.org) in the supporting information and by request. We thank two anonymous reviewers for their insightful comments and suggestions. We especially thank associates at the University of Sheffield (Jonathan Leake, Steve Banwart, and Megan Andrews) for their helpful discussion and implementation of the mesocosm system and assistance in greenhouse setup and maintenance from M.L. McCormack, S. DiLoreto, N. Bingham, and M. Davis. Logistical support and/or data were provided by the NSF-supported Susquehanna Shale Hills Critical Zone Observatory. We acknowledge all members of the SSHCZO who assisted in the sample collection and analyses especially J. Kissel, K. Gaines, J. Wubbels, and L. Smith. This study was supported by NSF grants to S.L.B. (EAR 1052614 and CHE 0431328 for the Center for Environmental Kinetics Analysis) and by NSF grant EAR 0725019 to C. Duffy (Pennsylvania State) for the SSHCZO.

References

Anderson, S. P., W. E. Dietrich, and G. H. Brimhall (2002), Weathering profiles, mass-balance analysis, and rates of solute loss: Linkages between weathering and erosion in a small, steep catchment, *Geol. Soc. Am. Bull.*, *114*(9), 1143–1158.

Andrews, D. M. (2011), Coupling dissolved organic carbon and hydropedology in the Shale Hills Critical Zone Observatory, PhD Dissertation, Dept. of Soil Science, The Pennsylvania State Univ., Univ. Park, Pa.

Andrews, D. M., H. Lin, Q. Zhu, L. Jin, and S. L. Brantley (2011a), Hot spots and hot moments of dissolved organic carbon export and soil organic carbon storage in the shale hills catchment, *Vadose Zone J.*, *10*(3), 943–954, doi:10.2136/vzj2010.0149.

Andrews, M. Y., J. R. Leake, B. G. Palmer, S. A. Banwart, and D. J. Beerling (2011b), Plant and mycorrhizal driven silicate weathering: Quantifying carbon flux and mineral weathering processes at the laboratory mesocosm scale, *Appl. Geochem.*, *26*, S314–S316.

Balogh-Brunstad, Z., C. K. Keller, B. T. Bormann, R. O'Brien, D. Wang, and G. Hawley (2008), Chemical weathering and chemical denudation dynamics through ecosystem development and disturbance, *Global Biogeochem. Cycles*, *22*, GB1007, doi:10.1029/2007GB002957.

Bergkvist, B., and L. Folkeson (1995), The influence of tree species on acid deposition, proton budgets, and element fluxes in south Swedish forest, *Ecol. Bull.*, *44*, 90–99.

Berner, E., R. Berner, and K. Moulton (2003), Plants and mineral weathering: Present and past, *Treatise on Geochem.*, *5*, 169–188.

Bormann, B. T., D. Wang, F. H. Bormann, G. Benoit, M. C. Snyder, R. April, and C. Michael (1998), Rapid, plant-induced weathering in an aggrading experimental ecosystem, *Biogeochemistry*, *43*(2), 129–155.

Boudissa, S. M., J. Lambert, C. Müller, G. Kennedy, L. Gareau, and J. Zayed (2006), Manganese concentrations in the soil and air in the vicinity of a closed manganese alloy production plant, *Sci. Total Environ.*, *361*(1–3), 67–72, doi:10.1016/j.scitotenv.2005.05.001.

Brantley, S. L., and M. Lebedeva (2011), Learning to read the chemistry of regolith to understand the critical zone, *Annu. Rev. Earth Planet. Sci.*, *39*, 387–416.

Brimhall, G. H., and W. E. Dietrich (1987), Constitutive mass balance relations between chemical composition, volume, density, porosity, and strain in metasomatic hydrochemical systems: Results on weathering and pedogenesis, *Geochim. Cosmochim. Acta*, *51*, 567–587.

Buck, C. S., W. M. Landing, J. Resing, and C. I. Measures (2010), The solubility and deposition of aerosol Fe and other trace elements in the North Atlantic Ocean: Observations from the A16N CLIVAR/CO2 repeat hydrography section, *Mar. Chem.*, *120*(1–4), 57–70, doi:10.1016/j.marchem.2008.08.003.

Chaney, R. L., M. Malik, Y. M. Li, S. L. Brown, E. P. Brewer, J. S. Angle, and A. J. Baker (1997), Phytoremediation of soil metals, *Curr. Opin. Biotechnol.*, *8*, 279–84.

Ciolkosz, E. J. (2000), Major and Trace Elements in Southwestern Pennsylvania Soils. Agronomy Series Number 148, The Pennsylvania State University.

Ciolkosz, E. J., and M. K. Amistadi (1993), Metals in Pennsylvania Soils. Agronomy Series Number 128, The Pennsylvania State University.

Ciolkosz, E. J., R. C. Stehouwer, and M. K. Amistadi (1998), Metals Data for Pennsylvania Soils. Agronomy Series Number 140, The Pennsylvania State University.

Cole, K. L., D. R. Engstrom, R. P. Futyma, and R. Stottlemyer (1990), Past atmospheric deposition of metals in northern Indiana measured in a peat core from Cowles Bog, *Environ. Sci. Technol.*, *24*(4), 543–549.

Dere, A. L., T. S. White, R. H. April, B. Reynolds, T. E. Miller, E. P. Knapp, L. D. McKay, and S. L. Brantley (2013), Climate dependence of feldspar weathering in shale soils along a latitudinal gradient, *Geochim. Cosmochim. Acta*, *122*, 101–126.

Drever, J. I. (1994), The effect of land plants on weathering rates of silicate minerals, *Geochim. Cosmochim. Acta*, *58*(10), 2325–2332, doi:10.1016/0016-7037(94)90013-2.

Duffy, C. J. (2012), CZO Dataset: Shale Hills - Streamflow / Discharge (2006-2012) - Shale Hills Stream Flow / Discharge Data. [Retrieved from http://criticalzone.org/shale-hills/data/dataset/3613/.]

Eissenstat, D., J. Wubbels, T. Adams, and J. Osborne (2013), Susquehanna Shale Hills Critical Zone Observatory Tree Survey (2008), Integrated Earth Data Applications (IEDA), doi:10.1594/IEDA/100268.

Filippelli, G. M., and M. A. S. Laidlaw (2010), The elephant in the playground: Confronting lead contaminated soils as an important source of lead burdens to urban populations, *Perspect. Biol. Med.*, *53*(1), 31–45.

Gardner, T. W., J. B. Ritter, C. A. Shuman, J. C. Bell, K. C. Sasowsky, and N. Pinter (1991), A periglacial stratified slope deposit in the valley and Ridge province of central Pennsylvania, USA: Sedimentology, stratigraphy, and geomorphic evolution, *Permafr. Periglac. Processes*, *2*, 141–162.

Herndon, E. M. (2012), Biogeochemistry of manganese contamination in a temperate forested watershed, PhD dissertation, The Pennsylvania State University.

Herndon, E. M., and S. L. Brantley (2011), Movement of manganese contamination through the critical zone, *Appl. Geochem.*, *26*, S40–S43, doi:10.1016/j.apgeochem.2011.03.024.

Herndon, E. M., L. Jin, and S. L. Brantley (2011), Soils reveal widespread manganese enrichment from industrial inputs, *Environ. Sci. Technol.*, *45*(1), 241–7, doi:10.1021/es102001w.

Herndon, E. M., C. E. Martínez, and S. L. Brantley (2014), Spectroscopic (XANES/XRF) characterization of contaminant manganese cycling in a temperate watershed, *Biogeochemistry*, *121*(3), 505–517.

Hokura, A., H. Matsuura, F. Katsuki, and H. Haraguchi (2000), Multielement determination of major-to-ultratrace elements in plant reference materials by ICP-AES/ICP-MS and evaluation of their enrichment factors, *Anal. Sci.*, *16*, 1161–1168.

Horsley, S. B., R. P. Long, S. W. Bailey, R. A. Hallett, and T. J. Hall (2000), Factors associated with the decline disease of sugar maple on the Allegheny Plateau, *Can. J. For. Res.*, *30*, 1365–1378.
Jin, L., D. M. Andrews, G. H. Holmes, H. Lin, and S. L. Brantley (2011), Opening the "black box": Water chemistry reveals hydrological controls on weathering in the Susquehanna Shale Hills Critical Zone Observatory, *Vadose Zone J.*, *10*(3), 928–942, doi:10.2136/vzj2010.0133.
Jobbagy, E. G., and R. B. Jackson (2004), The uplift of soil nutrients by plants: Biogeochemical consequences across scales, *Ecology*, *85*(9), 2380–2389.
Johnson, N. M., G. E. Likens, F. H. Bormann, D. W. Fisher, and R. S. Pierce (1969), A working model for the variation in stream water chemistry at the Hubbard Brook Experimental Forest, New Hampshire, *Water Resour. Res.*, *5*(6), 1353–1363.
Kabata-Pendias, A., and H. Pendias (2001), *Trace Elements in Soils and Plants*, 3rd ed., CRC Press LL, Boca Raton, Fla.
Kogelmann, W. J., and W. E. Sharpe (2006), Soil acidity and manganese in declining and nondeclining sugar maple stands in Pennsylvania, *J. Environ. Qual.*, *35*(2), 433–41, doi:10.2134/jeq2004.0347.
Kraepiel, A. M. L., A. L. Dere, E. M. Herndon, and S. L. Brantley (2015), Natural and anthropogenic processes contributing to metal enrichment in surface soils of central Pennsylvania, *Biogeochemistry*, doi:10.1007/s10533-015-0068-5.
Landre, A. L., S. A. Watmough, and P. J. Dillon (2010), Metal pools, fluxes, and budgets in an acidified forested catchment on the Precambrian shield, Central Ontario, Canada, *Water Air Soil Pollut.*, *209*, 209–228, doi:10.1007/s11270-009-0193-7.
Lerman, A., and L. Wu (2008), Kinetics of global geochemical cycles, in *Kinetics of Water-Rock Interaction*, pp. 655–736, Springer, New York, doi:10.1007/978-0-387-73563-4_13.
Li, J., D. D. Richter, A. Mendoza, and P. Heine (2008), Four-decade responses of soil trace elements to an aggrading old-field forest: B, Mn, Zn, Cu, and Fe, *Ecology*, *89*(10), 2911–2923.
Liermann, L. J., R. Mathur, L. E. Wasylenki, J. Nuester, A. D. Anbar, and S. L. Brantley (2011), Extent and isotopic composition of Fe and Mo release from two Pennsylvania shales in the presence of organic ligands and bacteria, *Chem. Geol.*, *281*, 167–180, doi:10.1016/j.chemgeo.2010.12.005.
Lin, H. S., W. Kogelmann, C. Walker, and M. A. Bruns (2006), Soil moisture patterns in a forested catchment: A hydropedological perspective, *Geoderma*, *131*, 345–368, doi:10.1016/j.geoderma.2005.03.013.
Lindberg, S. E., and R. C. Harriss (1983), Water and acid soluble trace metals in atmospheric particles, *J. Geophys. Res.*, *88*(C9), 5091–5100, doi:10.1029/JC088iC09p05091.
Lucchini, R. G., E. Albini, L. Benedetti, S. Borghesi, R. Coccaglio, E. C. Malara, G. Parrinello, S. Garattini, S. Resola, and L. Alessio (2007), High prevalence of Parkinsonian disorders associated to manganese exposure in the vicinities of ferroalloy industries, *Am. J. Ind. Med.*, *50*, 788–800, doi:10.1002/ajim.20494.
Lytle, C., B. Smith, and C. Z. McKinnon (1995), Manganese accumulation along Utah roadways: A possible indication of motor vehicle exhaust pollution, *Sci. Total Environ.*, *162*, 105–109, doi:10.1016/0048-9697(95)04438-7.
Ma, L., J. Konter, E. Herndon, L. Jin, G. Steinhoefel, D. Sanchez, and S. Brantley (2014), Quantifying an early signature of the industrial revolution from lead concentrations and isotopes in soils of Pennsylvania, USA, *Anthropocene*, doi:10.1016/j.ancene.2014.12.003, in press.
McCain, D. C., and J. L. Markley (1989), More manganese accumulates in maple Sun leaves than in shade leaves, *Plant Physiol.*, *90*, 1417–1421.
Miller, O. (1998), High-temperature oxidation: Dry ashing, in *Handbook and Reference Methods for Plant Analysis*, edited by Y. P. Kalra, CRC Press LLC, New York.
National Atmospheric Deposition Program (2011), National Atmospheric Deposition Program. [Available at http://nadp.sws.uiuc.edu/.]
National Research Council (Ed.) (1973), *Medical and Biological Effects of Environmental Pollutants: Manganese*, National Academy of Sciences, Washington, D. C.
Navrátil, T., J. B. Shanley, P. Skřivan, P. Krám, M. Mihaljevič, and P. Drahota (2007), Manganese biogeochemistry in a central Czech Republic catchment, *Water Air Soil Pollut.*, *186*, 149–165, doi:10.1007/s11270-007-9474-1.
Niu, X., K. A. Lehnert, J. Williams, and S. L. Brantley (2011), CZChemDB and EarthChem: Advancing management and access of critical zone geochemical data, *Appl. Geochem.*, *26*, S108–S111.
Nriagu, J., and J. Pacyna (1988), Quantitative assessment of worldwide contamination of air, water, and soils by trace metals, *Nature*, *333*, 134–139.
Pacyna, J. M., and E. G. Pacyna (2001), An assessment of global and regional emissions of trace metals to the atmosphere from anthropogenic sources worldwide, *Environ. Rev.*, *9*, 269–298, doi:10.1139/er-9-4-269.
Parekh, P. P. (1990), A study of manganese from anthropogenic emissions at a rural site in the eastern United States, *Atmos. Environ.*, *24A*(2), 415–421.
Rahn, K., and D. Lowenthal (1984), Elemental tracers of distant regional pollution aerosols, *Science*, *223*(4632), 132–139.
Rauch, J. N., and J. M. Pacyna (2009), Earth's global Ag, Al, Cr, Cu, Fe, Ni, Pb, and Zn cycles, *Global Biogeochem. Cycles*, *23*, GB2001, doi:10.1029/2008GB003376.
Rice, K. C., T. M. Scanlon, J. A. Lynch, and B. J. Cosby (2014), Decreased atmospheric sulfur deposition across the southeastern U.S.: When will watersheds release stored sulfate?, *Environ. Sci. Technol.*, *48*, 10,071–10,078.
Runkel, R., C. G. Crawford, and T. A. Cohn (2004), Load estimator (LOADEST): A FORTRAN program for estimating constituent loads in streams and rivers, in *Techniques and Methods Book 4*, edited by U. S. G. Survey, Reston, Va.
Scudlark, J. R., K. C. Rice, K. M. Conko, O. P. Bricker, and T. M. Church (2005), Transmission of atmospherically derived trace elements through an undeveloped, forested Maryland watershed, *Water Air Soil Pollut.*, *163*, 53–79.
Selin, N. E. (2009), Global biogeochemical cycling of mercury: A review, *Annu. Rev. Environ. Resour.*, *34*, 43–63.
Sen, I. S., and B. Peucker-Ehrenbrink (2012), Anthropogenic disturbance of element cycles at the Earth's surface, *Environ. Sci. Technol.*, *46*(16), 8601–8609.
Shanley, J. B. (1986), Manganese biogeochemistry in a small Adirondack forested lake watershed, *Water Resour. Res.*, *22*(12), 1647–1656, doi:10.1029/WR022i012p01647.
Smith, D. B., W. F. Cannon, L. G. Woodruff, F. Solano, J. E. Kilburn, and D. L. Fey (2013), Geochemical and mineralogical data for soils of the conterminous United States: U.S. Geological Survey Data Series 801, p. 19. [Available at http://pubs.usgs.gov/ds/801/.]
Smith, L. (2013), Aboveground carbon distribution across a temperate watershed, MS thesis, The Pennsylvania State University.
St. Clair, S. B., and J. P. Lynch (2005), Element accumulation patterns of deciduous and evergreen tree seedlings on acid soils: Implications for sensitivity to manganese toxicity, *Tree Physiol.*, *25*, 85–92.
Taylor, L. L., J. R. Leake, J. Quirk, K. Hardy, S. Banwart, and D. Beerling (2009), Biological weathering and the long-term carbon cycle: Integrating mycorrhizal evolution and function into the current paradigm, *Geobiology*, *7*, 171–91, doi:10.1111/j.1472-4669.2009.00194.x.
Turekian, K. K., and K. H. Wedepohl (1961), Distribution of the elements in some major units of the Earth's crust, *Geol. Soc. Am. Bull.*, *72*, 175–192.
U.S. Environmental Protection Agency (1984), Health assessment document for manganese (pp. EPA 600/8–83–013F), Cincinatti, Ohio.

U.S. Environmental Protection Agency (1985), Locating and estimating air emissions from sources of manganese (pp. EPA–450/4–84–007h).
U.S. Geological Survey (2014), USGS water data for the nation. [Available at http://waterdata.usgs.gov/nwis.]
Watmough, S. A., M. C. Eimers, and P. J. Dillon (2007), Manganese cycling in central Ontario forests: Response to soil acidification, *Appl. Geochem.*, *22*, 1241–1247.
Williams, P. T., M. Radojevic, and A. G. Clarke (1988), Dissolution of trace metals from particles of industrial origin and its influence on the composition of rainwater, *Atmos. Environ. (1967)*, *22*(7), 1433–1442, doi:10.1016/0004-6981(88)90168-0.
Wubbels, J. K. (2010), Tree species distribution in relation to stem hydraulic traits and soil moisture in a mixed hardwood forest in central Pennsylvania, MS thesis, Dept. of Horticulture, The Pennsylvania State Univ., Univ. Park, Pa.